Computer Methods in Biomechanics and Biomedical Engineering
Vol. 12, No. 3, June 2009, 333–339

Taylor & Francis
Taylor & Francis Group

Biomechanical evaluation of porous biodegradable scaffolds for revision knee arthroplasty

Alexandre Terrier*, Marjan Sedighi-Gilani[1], Alireza Roshan Ghias[2], Line Aschwanden[3] and Dominique P. Pioletti[4]

Laboratory of Biomechanical Orthopedics, Ecole Polytechnique Federal de Lausanne, Lausanne, Switzerland

(*Received 23 July 2008; final version received 5 November 2008*)

Tibial bone defect is a critical problem for revision knee arthroplasty. Instead of using metallic spacer or cement, biodegradable scaffolds could be an alternative solution. A numerical model of a revision knee arthroplasty was thus developed to estimate the mechanical resistance of the scaffold in this demanding situation. The tibia, scaffold, and prosthesis were represented by simplified parameterised geometries. The maximal gait cycle force was applied asymmetrically to simulate a critical loading. Several parameters were analysed: 1) inter-individual variability, 2) cortical bone stiffness, 3) cortical bone thickness, 4) prosthesis fixation quality, and 5) scaffold thickness. The calculated scaffold strain was compared to its experimental ultimate strain. Among the tested parameters, failure was only predicted with scaffold thickness below 5 mm. This study suggests that biodegradable bone scaffolds could be used to fill bone defects in revision knee arthroplasty, but scaffold size seems to be the limiting factor.

Keywords: bone scaffold; prosthesis; knee; revision arthroplasty

1. Introduction

In case of failure of primary knee prosthesis, a revision knee arthroplasty (RKA) is required. During the removal of the primary prosthesis, a part of the bone that was in contact with the prosthesis is usually damaged (Huff and Sculco 2007). For these revision prostheses, initial stability is a key issue because of the loss of bone support. In general, this stability is achieved by using longer stems, either for the tibial or femoral components (Bugbee et al. 2001). The stem used in the tibial part is cemented or press-fitted inside the medullary canal (Completo et al. 2008; Kim et al. 2008). Although the RKA is quite common, its success rate is not as good as the primary fixation (Su et al. 2000). When a successive revision is required, the bone defect becomes even more critical. It would then be especially important to use a material to fill the defect which could be replaced at term by the bone of the patient. To this end, a biodegradable material should be used.

However, the bone defects are usually replaced either with bone grafts (autografts, allografts and xenografts), metallic augments, cement (Stockley et al. 1992; Mow and Wiedel 1996; van Loon et al. 1999; Completo et al. 2008). Each one of these substitutes has certain advantages and disadvantages. Autografts are the gold standard, since they are fresh, vascularised and seeded naturally with the patient's own cells. However, the use of autologous bone has been hampered by its short supply and the pain and long-term discomfort that accompany such harvests from the iliac crest (Stevens et al. 2005). Allografts and xenografts allow ingrowth of bone and restoring bone stock, are easy to shape, and are relatively cheap, but there is always a risk of viral disease transfer from the donor to the host (Boyce et al. 1999). Metallic augments, on the other hand, provide excellent mechanical properties, but they do not biologically restore the bone stock and they usually require additional bone removal, although minimal, to make the pattern of bone loss encountered match exactly the configuration of the augment (Huff and Sculco 2007a, 2007b; Mabry and Hanssen 2007). Therefore, there is a need for a bone substitute that overcomes these limitations, and tissue engineered bone substitutes have been proposed (Yaszemski et al. 1996).

There are basically two major options for biodegradable scaffold: ceramic or polymer. The ceramic, usually made of calcium-phosphate, may be delicate to use in such demanding mechanical environment as they present a brittle behaviour. The polymers, such as PLA or PLGA, on the other hand are ductile but may not have enough mechanical properties to withstand the load. If the polymer scaffolds have enhanced mechanical properties, they may be an ideal material for bone substitute in case of RKA.

Recently, a synthetic bone substitute made of PLA/5% β-tri-calcium-phosphate (β-TCP) and processed by supercritical CO_2 foaming has been developed for various clinical applications (Mathieu et al. 2006). The biocompatibility of this polymer–ceramic composite has been tested with human primary osteoblasts (Montjovent et al. 2005). In addition, the behaviour of this bone substitute has been evaluated *in vivo* in a critical size defect craniotomy model in rats and bone bridging could be seen 18 weeks after

*Corresponding author. Email: alexandre.terrier@epfl.ch

ISSN 1025-5842 print/ISSN 1476-8259 online

DOI: 10.1080/10255840802603589
http://www.informaworld.com

implantation (Montjovent et al. 2007). This bone scaffold might thus be a suitable candidate as a bone substitute in RKA. The principal limitation in the use of this scaffold would be its mechanical resistance to the high loading present within the knee joint during typical activities such as walking.

Therefore, the objective of this study was to estimate the maximal stains that would support a composite artificial bone scaffold in RKA. For this purpose, a 3D finite element model was developed and the effect of different geometrical and mechanical parameters on the scaffold strain was investigated. The analysed parameters were the tibia geometry and mechanical properties, the bone defect size, and the prosthesis fixation quality. The calculated strain was compared to the experimental ultimate (collapse) strains.

2. Materials and methods

To test the relative importance of each parameter considered here on the mechanical failure of the bone scaffold, we developed a simplified 3D numerical model of the tibia after revision surgery (Figure 1). This model was composed of the tibia, the bone scaffold and the revision prosthesis. Three tibias were reconstructed from patients' CT data. For each tibia, a bone defect was simulated, filled with a bone scaffold, and completed by a revision knee prosthesis. A critical loading was applied to the tibial plate of the prosthesis. The parameters considered here were varied to check their effect on the strain within the scaffold. The calculated strain was then compared to the experimental ultimate (collapse) strain.

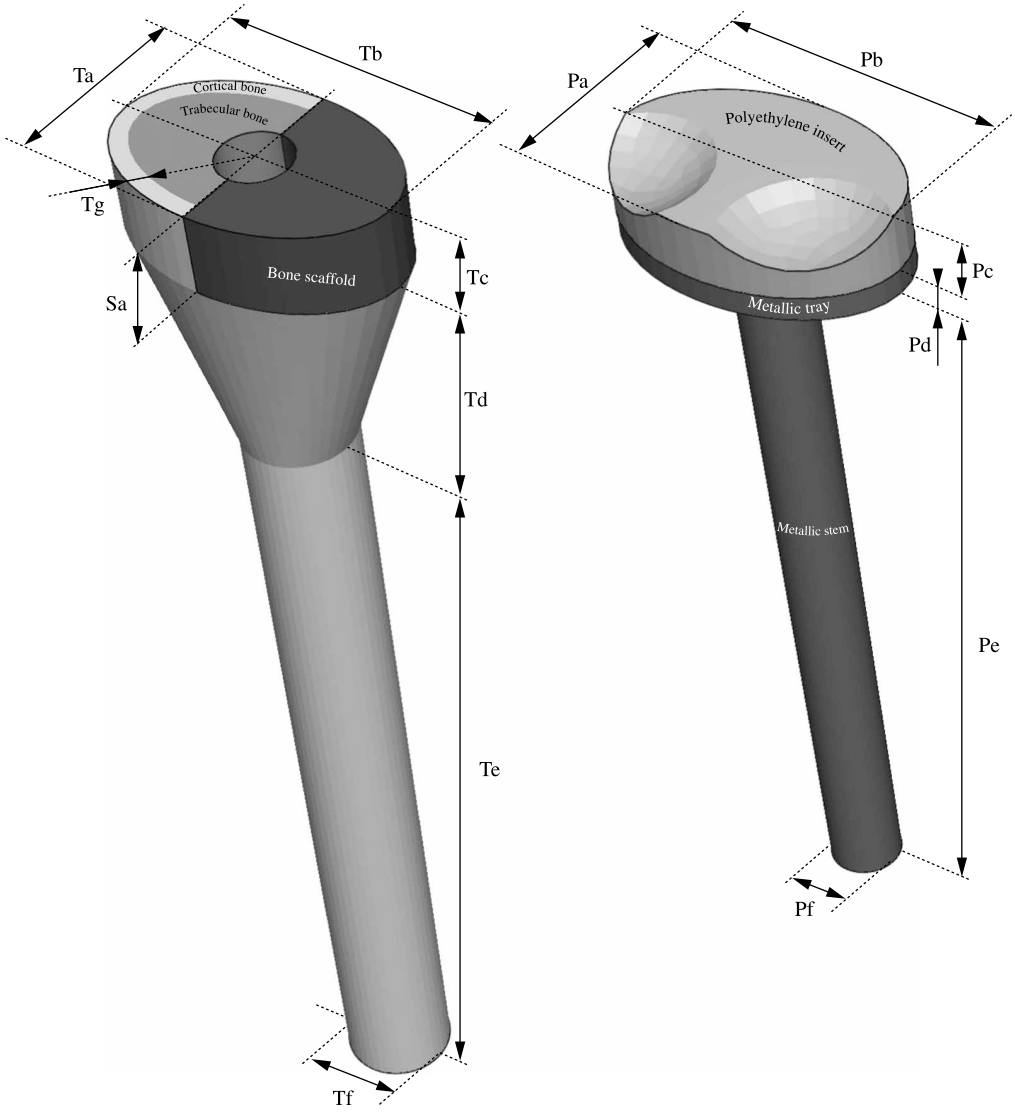

Figure 1. The revised tibia was modeled by a simplified geometry of the tibia, the artificial bone scaffold (left), and the revision knee prosthesis (right). The dimension values are given in Table 1.

Table 1. The parameters of the simplified geometry of the three tibias A, B and C were measured from CT data and are reported in this table.

	Ta	Tb	Tc	Td	Te	Tf	Tg	Sa	Pa	Pb	Pc	Pd	Pe	Pf
A	45	67	16	36	266	33	6	18	45	67	12	5	170	21
B	48	69	18	28	283	29	6	16	48	69	12	5	170	17
C	42	65	18	50	200	25	6	18	42	65	12	5	170	16

The parameters are illustrated in Figure 1. The dimensions of the bone scaffold and prosthesis were adapted to each tibia.

2.1 Tibia

In order to study the effect of inter-individual geometry and mechanical properties of the tibia, three different models were built. These models were reconstructed from CT images. The diaphysis was a hollow cylinder and the epiphysis was a cut cone connected to an elliptical cylinder on top (Figure 1). The diaphysis was composed of cortical bone, while the epiphysis was composed of both cortical and trabecular bone. Seven parameters were used to characterise the simplified tibial geometry (Table 1). The Young's modulus of cortical bone and trabecular bone were 20.7 and 770 MPa, respectively (Rho et al. 1995). The Poisson's ratios of cortical and trabecular bone were 0.3.

2.2 Bone scaffold

The bone defect was assumed to be a segmental defect (Huff and Sculco 2007), in only one side of the epiphysis. Its geometry was an elliptical shape, filling perfectly the gap between the tibial metaphysis and the tibial component. The scaffold was a matrix of poly(L-lactic) acid and a ceramic filler of β-TCP (at 5%). The mechanical characteristics of the bone scaffold were measured experimentally: the porosity was 83%, the Young's modulus was 80 MPa, the Poisson's ratio was 0.3 and the ultimate compressive (collapse) strain was 2.9% (Mathieu 2004; Mathieu et al. 2006).

2.3 Prosthesis

The simplified geometry of the prosthesis was adapted from a revision knee prosthesis prototype, which is derived from the FIRST prosthesis (Symbios Orthopédie SA, Switzerland). This prosthesis is an ultra-congruent mobile bearing and postero-stabilised total knee prosthesis. The simplified geometry of the prosthesis was composed of a cylindrical metallic stem and an elliptical metallic tray (perfectly fitting the tibial cut). The radius of the cylindrical stem was calculated to have the same second moment of area (resistance to bending) as the real stem. To assess the estimation of this radius, the bending properties of the simplified prosthesis was compared to the un-simplified prosthesis. For this comparison, the same bending moment was applied on both the simplified and un-simplified prostheses, and the lateral displacement was calculated and compared. The polyethylene insert had also an elliptical basis, where the two spherical surfaces represented each condyle (Figure 1). The center and radius of the spherical surfaces matched exactly to the prototype. The femoral component was simply represented by two spherical surfaces, with center and radius that correspond to the real femoral component. All metal parts were Co–Cr alloy, with a Young's modulus of 210 GPa and Poisson's ratio of 0.33. The polyethylene insert had a Young's modulus of 500 MPa and Poisson's ratio of 0.4. The femoral component surfaces were rigid.

2.4 Boundary conditions

A force of 3.5 times of the body weight was considered as the maximum load applied to the knee during the gait cycle (Hurwitz et al. 1998). The body weight was estimated to be 857 N, from patients with RKA (Hockman et al. 2005). An asymmetrical loading was simulated, corresponding to the worse case scenario of an unbalanced loading on the side of the bone defect. Thus, 3000 N were applied on the defect side of the tibia through the femoral component. The distal end of the tibia was completely constrained.

For the comparison between the simplified and un-simplified prosthesis, the same conditions were applied, but on the prosthesis only, without the tibia.

2.5 Numerical issues

The numerical analyses were performed with the implicit solver of Abaqus software (Stimuli, Pawtucket, RI, USA). Linear hexahedral elements were used for all components of the model, except for the femoral component, which was represented by rigid analytical surfaces. The interface between the femoral component and the polyethylene insert were standard hard contact. All other interfaces were completely tied, except around the stem for the fixation. To ensure the independency of the results from the mesh size, a mesh sensitivity analysis was done. Three average mesh sizes were tested and compared: 2.5, 2 and 1.5 mm. For the comparison between the simplified and un-simplified prosthesis, the complex geometry of the un-simplified prosthesis was filled with quadratic tetrahedral elements.

2.6 Parameter study

Five parameters were considered. The first one was the inter-individual variability of the geometrical properties of the tibia. In fact, for this first parameter analysis, several geometrical parameters of the tibia were actually changed simultaneously, according to CT images of three tibias. The other four parameters were varied on one tibia.

2.6.1 Inter-individual variability

Three different tibias were reconstructed, using the simplified parameterised geometry described above. All dimensions of the parameterised tibia were estimated from CT images using Amira (www.amiravis.com). The parameters associated to each patient are given in Table 1.

2.6.2 Cortical bone stiffness

The cortical bone stiffness was changed drastically, from the reference value of 20.7 to 15, 10 and 5 GPa.

2.6.3 Cortical bone thickness

The thickness of the cortical bone was varied by changing the external radius of the cortical wall from 4 to 6 mm (the reference) and 8 mm.

2.6.4 Stem fixation

For the reference case, the interface between the stem prosthesis and the bone (cortical, trabecular and scaffold) were fully bonded. To test the effect of the fixation quality, the interface was partly and progressively debonded along

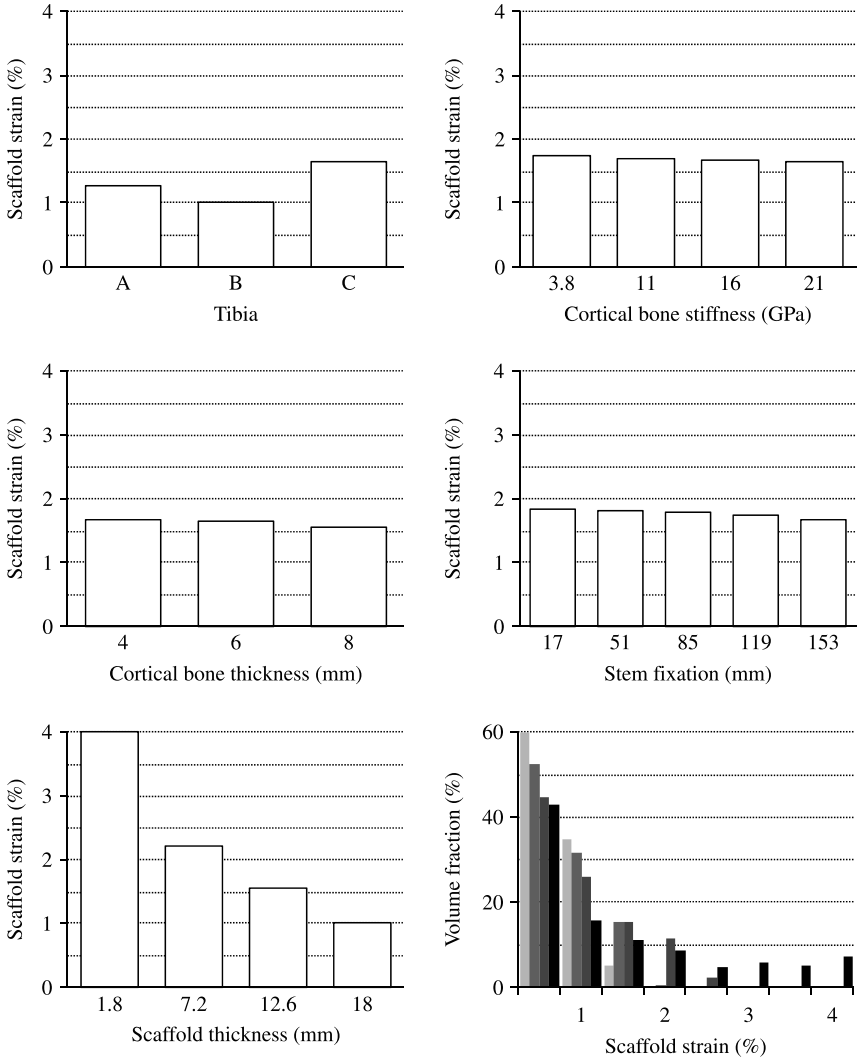

Figure 2. Maximum value of the minimum principal strain (compression) within the artificial bone scaffold for the parameter considered here: (1) tibia inter-variability, (2) cortical bone stiffness, (3) cortical bone thickness, (4) stem fixation and (5) scaffold thickness. The last graph represents the volumetric distribution of the strain within the scaffold for the four scaffold thicknesses (higher thickness corresponds to darker gray level).

the stem, from the proximal to the distal part. The fixation length was 153 mm (fully bonded), 119 mm, 85 mm, 51 mm, or only 17 mm.

2.6.5 Scaffold thickness

The scaffold section shape was constrained to fit the elliptical shape of the tibial metaphysis, but different scaffold thicknesses were considered, from 16 mm (the reference) to 11.2 mm, 6.4 mm and 1.6 mm.

3. Results

All results of the study parameters are presented as the maximal value of the minimal principal strain (compression) within the scaffold (Figure 2). For the last parameter, the scaffold thickness, the volumetric distribution of the strain was presented in a histogram.

3.1 Numerical issues

The three element sizes tested had very little influence on the results. The changes in the volume fraction of different strain levels were indeed modified by less than 1%. The pure bending test on the un-simplified prosthesis resulted in an absolute displacement of 891 μm, while it was 863 μm on the simplified prosthesis.

3.2 Inter-individual variability

The strain distribution within the bone scaffold was rather similar for each tibia. The maximum value of the strain within the whole scaffold was indeed between 1 and 1.7% for the three tibia tested.

3.3 Cortical bone stiffness

The effect of the cortical bone thickness was very low. The maximum variation from the reference of 21 GPa was less than 5% at 3.8 GPa. In that case, the maximum strain remained below 2%.

3.4 Cortical bone thickness

Decreasing the cortical thickness by 2 mm from the reference value of 6 mm increased the maximal stain by less than 1%. Increasing the cortical thickness by 2 mm from the reference value of 6 mm decreased the maximal strain by more than 6%.

3.5 Stem fixation

The quality of the stem fixation also had a limited influence on the scaffold strain. Between the fully bonded stem and the most critical fixation case considered here, the increase of the maximal strain was less than 9% and the maximal strain was still below 2%.

3.6 Scaffold thickness

Among the parameters considered here, the scaffold thickness had the most important effect on the scaffold strain. From the reference value of 18 mm, the maximal strain exceeded 2% with the thickness of 7.2 mm and 4% with a thickness of 1.8 mm. A simple interpolation from 7.2 to 1.8 mm thickness predicts that the maximal strain would reach the failure strain of 2.9% for a scaffold thickness of 5 mm. A more detailed description of the scaffold strain was analysed by calculating the volumetric distribution of the strain by 0.5 increments (last graph of Figure 2). This graph also showed the increase of strain as the scaffold thickness decreased (light grey to dark gray). In the worst case (1.8 mm), about 15% of the scaffold volume reached the strain limit.

4. Discussion

During the RKA, large bone defect can be a challenging problem for the surgeon. Various solutions are used to fill the gaps between the revision implant and the remaining bone, but the possibility of using artificial bone scaffolds that eventually transform into healthy bone is still unclear. In this study, finite element methods were used to estimate the mechanical resistance of such a scaffold during typical loading of a tibial component. This numerical study predicted that use of an artificial bone scaffold might be an alternative to fill bone defects in RKA. The main limitation in the use of these scaffolds was the size of the scaffold, which should not be lower than 5 mm to prevent the collapse of the scaffold. The above criterion assumes a good fixation of the stem to the distal tibia.

To study the inter-individual variability of the tibial geometry on the scaffold strain, three tibias were reconstructed from CT images. For each tibia, the maximal strain inside the bone scaffold was lower than the experimental collapse strain. To extend the range of this three-specimen test, the cortical stiffness and cortical thickness were arbitrarily changed to extreme values, but there was still a limited effect on the scaffold strain. The fixation quality of the stem, which was expected to be an important factor, had also little effect on the scaffold strain, even when only the very last distal portion of the stem was bonded to the intramedular canal. These results reveal that the joint load is directly transferred from the tibial tray to the distal tibia, through the metallic stem (stress shielding). Actually, only the parameter associate to the scaffold geometry could bring the scaffold strain above the collapse limit. This result also makes sense because of the stress shielding of the metallic stem. Since the displacement of the external faces of the scaffold were indeed more or less

constant (mainly dependant on the stem rigidity), the strain increased as the scaffold dimension decreased. This study was focused on the mechanical failure of the scaffold, but the strain distribution gives some insight into the osteogenic response that can be expected. It has indeed been reported that scaffold strain of the order of 1% promotes cell ingrowth and extracellular matrix synthesis (Wood et al. 2006).

The simplicity was the main advantage of this model. It provided a sensitive analysis of the hypothetical important parameters that can influence the mechanical failure of the scaffold. This analysis was indeed much easier that an equivalent analysis on cadaver knees, which would be however required at some point to confirm these numerical predictions. Nevertheless, it was very useful to have this first rough estimate of the importance of the main parameters that can provoke an immediate failure of the scaffold. The advantage of the simplicity was counter-balanced by several limitations. Current scaffolds are either made of ceramics or polymers. Ceramics tend to be too brittle (break) and polymer too soft (collapse). In comparison with ceramic scaffolds, the scaffold used here is a combination of both materials and has a more ductile behaviour (Mathieu 2004). However, for this preliminary study, the progressive failure caused by cyclic fatigue was not considered here. There was in fact no experimental data on the fatigue of this specific scaffold. For that reason, we choose to compare the minimal principal strain with the ultimate (collapse) strain, which was measured experimentally. We may however expect that the fatigue criterion would be of course lower than the ultimate strain criterion. It remains difficult to extrapolate further since we also expect that new bone would form into the scaffold. Anyway, the results presented here must be regarded as upper limits that should certainly be further investigated. The loading case was a simple static value estimated from the gait cycle. This loading is however a rather good estimation of the maximal force that can be applied on the knee joint during the first weeks following a revision knee surgery. Although the patient is usually asked (and trained) to not exceed 10% of the bodyweight (≈ 80 N) on the operated leg, it is clear that this rule cannot always be satisfied. Besides, it is also not known when the scaffold will be regenerated into host bone. Although muscles are known to have an important effect on knee biomechanics, there were not accounted for in this study. We assumed however that they would not change drastically the scaffold strain, because of its lateral position, away from the line of action of the quadriceps.

The present model was rather simple, but still relevant for the proposed analysis. The bone strains predicted here reached approximately 1500 microstrains below the stem, 1000 along the stem and 100 under the baseplate. The bone strains after knee arthroplasty with long stems (revision surgery) have been measured in cadaveric bones (Reilly et al. 1982; Bourne and Finlay 1986; Jazrawi et al. 2001), synthetic bones (Completo et al. 2008) and numerical models (Completo et al. 2007). A strict comparison with the above more realistic models was rather difficult because of the different experimental conditions. However, these studies also reported a stress shielding effect (stress/strain decrease) above the stem. The level of strain was also comparable.

Within its limitations, this study assessed the feasibility of using composite bone scaffolds in a hybrid scaffold-prosthesis solution for RKA, particularly for the tibial component. We showed that the initial stability of the tibial component must still be achieved by the stem, and will never be supported in any way by the scaffold. Assuming that this initial stability is present, we also showed that collapse strain could be avoided, if the scaffold size is not below some critical values. These conclusions will have to be confirmed by a more realistic model of the tibia and implant, which should also provide a better estimation of the osteogenic level of the strain. Whatever the mechanisms at the cellular level, strain level within the scaffold matrix is indeed crucial in the process of bone ingrowth into such biodegradable polymer scaffolds (Wood et al. 2006; Duty et al. 2007).

Acknowledgements

This study was supported by the Swiss National Science Foundation (FNRS 205320-113408). The authors also thank Vincent Leclercq (R&D director at Symbios) for his help is designing this study.

Notes

1. Email: marjan.sedighigilani@gmail.com
2. Email: alireza.roshanghias@epfl.ch
3. Email: line.aschwanden@epfl.ch
4. Email: dominique.pioletti@epfl.ch

References

Bourne RB, Finlay JB. 1986. The influence of tibial component intramedullary stems and implant-cortex contact on the strain distribution of the proximal tibia following total knee arthroplasty. An *in vitro* study. Clin Orthop Relat Res. (208):95–99.

Boyce T, Edwards J, Scarborough N. 1999. Allograft bone. The influence of processing on safety and performance. Orthop Clin North Am. 30(4):571–581.

Bugbee WD, Ammeen DJ, Engh GA. 2001. Does implant selection affect outcome of revision knee arthroplasty? J Arthroplasty 16(5):581–585.

Completo A, Fonseca F, Simoes JA. 2007. Finite element and experimental cortex strains of the intact and implanted tibia. J Biomech Eng. 129(5):791–797.

Completo A, Simoes JA, Fonseca F, Oliveira M. 2008. The influence of different tibial stem designs in load sharing and stability at the cement–bone interface in revision TKA. Knee 15(3):227–232.

Duty AO, Oest ME, Guldberg RE. 2007. Cyclic mechanical compression increases mineralization of cell-seeded polymer scaffolds *in vivo*. J Biomech Eng. 129(4):531–539.

Hockman DE, Ammeen D, Engh GA. 2005. Augments and allografts in revision total knee arthroplasty: usage and outcome using one modular revision prosthesis. J Arthroplasty 20(1):35–41.

Huff TW, Sculco TP. 2007. Management of bone loss in revision total knee arthroplasty. J Arthroplasty 22(7):32–36.

Hurwitz DE, Sumner DR, Andriacchi TP, Sugar DA. 1998. Dynamic knee loads during gait predict proximal tibial bone distribution. J Biomech. 31(5):423–430.

Jazrawi LM, Bai B, Kummer FJ, Hiebert R, Stuchin SA. 2001. The effect of stem modularity and mode of fixation on tibial component stability in revision total knee arthroplasty. J Arthroplasty 16(6):759–767.

Kim YH, Kwon OS, Kim KK. 2008. Analysis of biomechanical effect of stem-end design in revision TKA using digital Korean model. Clin Biomech. 23(7):853–858.

Mabry TM, Hanssen AD. 2007. The role of stems and augments for bone loss in revision knee arthroplasty. J Arthroplasty 22(4 Suppl 1):56–60.

Mathieu L. 2004. Processing of porous polymer composites for bone tissue engineering. Mater Sci, Lausanne, EPFL. PhD.

Mathieu LM, Mueller TL, Bourban PE, Pioletti DP, Muller R, Manson JA. 2006. Architecture and properties of anisotropic polymer composite scaffolds for bone tissue engineering. Biomaterials 27(6):905–916.

Montjovent MO, Mathieu L, Hinz B, Applegate LL, Bourban PE, Zambelli PY, Manson JA, Pioletti DP. 2005. Biocompatibility of bioresorbable poly(L-lactic acid) composite scaffolds obtained by supercritical gas foaming with human fetal bone cells. Tissue Eng. 11(11–12):1640–1649.

Montjovent MO, Mathieu L, Schmoekel H, Mark S, Bourban PE, Zambelli PY, Laurent-Applegate LA, Pioletti DP. 2007. Repair of critical size defects in the rat cranium using ceramic-reinforced PLA scaffolds obtained by supercritical gas foaming. J Biomed Mater Res A. 83A:41–51.

Mow CS, Wiedel JD. 1996. Structural allografting in revision total knee arthroplasty. J Arthroplasty 11(3):235–241.

Reilly D, Walker PS, Ben-Dov M, Ewald FC. 1982. Effects of tibial components on load transfer in the upper tibia. Clin Orthop Relat Res. 165:273–282.

Rho JY, Hobatho MC, Ashman RB. 1995. Relations of mechanical properties to density and CT numbers in human bone. Med Eng Phys. 17(5):347–355.

Stevens MM, Marini RP, Schaefer D, Aronson J, Langer R, Shastri VP. 2005. *In vivo* engineering of organs: the bone bioreactor. Proc Natl Acad Sci USA 102(32):11450–11455.

Stockley I, McAuley JP, Gross AE. 1992. Allograft reconstruction in total knee arthroplasty. J Bone Joint Surg Br. 74(3):393–397.

Su DH, Chan CW, Seow KH, Lo NN, Yeo SJ, Tay BK, Tan SK. 2000. Results of revision total knee arthroplasty. Singapore Med J. 41(1):6–8.

Wood MA, Yang Y, Thomas PB, Haj AJ. 2006. Using dihydropyridine-release strategies to enhance load effects in engineered human bone constructs. Tissue Eng. 12(9):2489–2497.

Yaszemski MJ, Payne RG, Hayes WC, Langer R, Mikos AG. 1996. *In vitro* degradation of a poly(propylene fumarate)-based composite material. Biomaterials 17(22): 2127–2130.

van Loon CJ, de Waal Malefijt MC, Verdonschot N, Buma P, van der Aa AJ, Huiskes R. 1999. Morsellized bone grafting compensates for femoral bone loss in revision total knee arthroplasty. An experimental study. Biomaterials 20(1): 85–89.